

Influence of orientation and temperature on the fatigue crack growth of directionally solidification superalloys DZ125

Yi Shi^{1,*}, Xiaoguang Yang¹, Didi Yang¹, Guolei Miao² and Duoqi Shi¹

¹School of Energy and Power Engineering, Beihang University, 100191 Beijing, China

²Chengdu Holy Industry & Commerce Corp.LTD, 611936, Sichuan Province, China

Abstract. The influence of orientation and temperature on the fatigue crack growth of a directionally solidification superalloys named DZ125 were investigated in this study. The specimens were designed based on ASTM E647 standard and the compliance method was employed to monitor the crack growth. Tests were conducted at room temperature, 760°C and 850°C respectively. The longitudinal and transverse orientation were both studied in this tests. Results show that the orientation dependence is weak at elevated temperature compared with that at room temperature. However, the temperature influences the fatigue crack growth rate significantly and the largest difference can be an order of magnitude on the $da/dN-\Delta K$ graph. But the reduction in higher ΔK area of elevated temperature can still be observed. Potential reasons and hypothesis were explained in this paper. In addition, the crack growth mode appears to transfer from type I with the increase of temperature which also reflects the influence of temperature.

1 Introduction

DZ125 is a Chinese made nickel based directionally solidification superalloys, which is similar to the Rene'125 in USA. Due to its good resistance to creep and excellent strength at elevated temperature, it is applied for blades and vanes of advanced aero-engine^[1]. However, the working condition of turbine blades is so harsh that it is close to the materials' capability limit. To ensure the safety of operation, understanding the behavior of fatigue crack growth at elevated temperature is important for design and maintenance. Many previous studies focused on DZ125's behavior of low cycle fatigue life at elevated temperature^[2-3], TMF^[4], and environment and coating influence^[5-6] by conducting experiments on smooth cylinder specimen, while less efforts are put on the fatigue crack growth behavior of DZ125. Other directionally solidification material like IN738, GTD-111's fatigue crack growth behavior were studied.

This study aims at investigating the influence of orientation and temperature on the fatigue crack growth behaviour of DZ125. The fatigue crack growth rates were obtained by conducting experiments and the crack growth path was also compared to analyze the temperature and orientation effects.

2 Experiment

2.1 Material and specimen

The material was subjected to the following heat treatment: 1180°C/2 h→1230 °C/3 h, AC + 1100 °C/4 h, AC + 870 °C/20 h, and AC (AC: air cooling) before machined. The nominal chemical composition is presented in **Table. 1** and mechanical properties at different temperature are listed in **Table. 2**.

All the test specimens were machined from three pads whose dimension was 2000×60×20mm. The directional solidification direction was shown in **Fig. 1**. The compact tension (CT) specimens, shown in **Fig. 2** were designed based on the ASTM E647 standard^[7], with 50mm wide and 10mm thick. The notch length of the CT specimen is $a_0=8\text{mm}$. They specimens are divided into two groups, T and L. For the loading direction is parallel to the directionally solidification direction, these specimens are denoted as L-CT. While for the loading direction is perpendicular to the directionally solidification direction, such specimens are denoted as T-CT, as shown in **Fig. 1**. In addition, to accommodate the extensometer, the knife edge at the side of CT specimen for elevated temperature is different from that of a room temperature specimen.

2.2 Test method

In this study, the compliance method was applied to monitor the length of crack according to ASTM E647.

*Corresponding author: shiyi_sepe@buaa.edu.cn

The definition of compliance, $c = \delta/P$, is the instantaneous ratio between displacement and load [8], which is also the reciprocal of the stiffness D . Also, the compliance would remain constant until the crack has new advance. The compliance value increases with the crack growth, which also indicates the degraded resistance to the external load. At the premise of linear condition, such relationship can be analytically

expressed in a dimensionless value, $(EvB/P, E$ is the elastic modulus, v is the displacement between measurement points, B is the specimen thickness and P is force) and later is correlated to the crack length, which is similar to the potential drop method [9]. The theoretical compliance expression for CT specimen is given in the E647 standard, see equation (1)

$$a/W = N_0 + N_1U + N_2U^2 + N_3U^3 + N_4U^4 + N_5U^5 \tag{1}$$

Where: $U = 1/\left[A\frac{1}{2} + 1\right]$; $A = \epsilon EBW/P$; $N_0 = 1.0033$; $N_1 = -2.35$; $N_2 = 1.3694$; $N_3 = -15.294$; $N_4 = 63.182$; $N_5 = -74.42$, for $0.2 < a/W < 0.95$

Table 1. Nominal chemical compositions of DZ125 (wt. %)

Ni	C	Cr	Co	W	Mo	Al	Ti	Ta	B	Hf
Bal	0.096	8.77	9.88	7.29	2.00	5.13	1.03	3.70	0.015	1.42

Table 2. Material tensile properties

Orientation	Longitude				Transverse			
	20	760	850	900	20	760	850	900
Temperature(°C)	20	760	850	900	20	760	850	900
Young's modulus (GPa)	125.5	99.5	91.0	82.0	152.5	115.5	117.0	110.0
Tensile strength (MPa)	1220	1200	1040	860	990	940	915	810
0.2% offset yield strength (MPa)	915	960	825	635	815	730	760	625
Elongation (%)	11.0	13.0	16.0	19.0	13.0	9.7	9.0	8.7
Reduction in area (%)	12.5	20.0	21.0	26.0	20.0	26.0	24.0	23.0

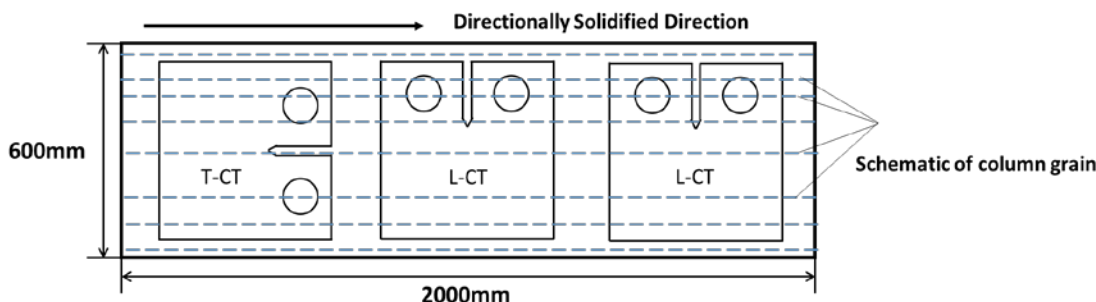


Fig. 1. The schematic of spemien[s] cut from a tab

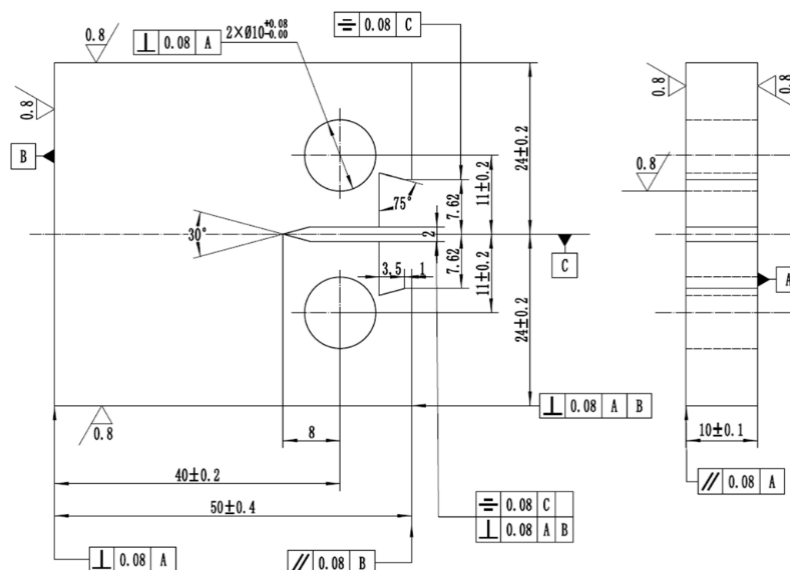


Fig. 2. The geometry of the compact tension specimen

The optical method was not utilized in this study due to the extremely high temperature. According to the physical law: anything will emit various radiation at any temperature. When the surface temperature is below 500 °C, it mainly emits infrared light with longer wave length. Generally, the sensor of camera is not sensitive to the long wave length. Therefore, there will be no influence on the brightness of the captured images. However, with the temperature increases, the corresponding wavelength shifts to shorter area which falls into the sensitive area of the sensor. Thus, the image will be too bright to observe and measure the crack length^[10].

2.3 Experimental Procedure

All the fatigue crack growth tests were conducted on the MTS 370 servo-hydraulic system. The load was monitored by the system load cell. Prior to the fatigue crack growth test, all specimens were pre-cracked for 1mm at room temperature to ensure the shape of crack inside meets the corresponding requirement. Then the knife edge was machined to accommodate the extensometer. The gage whose length was 15.2mm and the diameter was 5mm was assembly at the knife edge of the specimen. This is designed to extend to the furnace, shown in **Fig. 3**. To ensure the accuracy of

measurement, moderate cyclic loading was applied and the gage was adjusted until the curve of COD and force was approximately two close line during the loading and unloading stage, shown in **Fig. 4**. Some space is left for the tip of the rod and the knife edge considering the expansion of specimen after heating.

Later, the specimens were heated in a resistance-type furnace and center- temperature of the notch was measured by the thermal-couples. The specimens were set at minimum loading during the heating process and they were soaked at the expected temperature for 1h before the fatigue crack growth test. The thermal gradient was strictly controlled below 5 °C and the response of COD was also checked under cyclic loading.

The condition of fatigue tests were shown in **Table. 3**. The maximum loading ranges from 8.6kN to 9.4 kN and the reason for this difference will be explained later. The test frequency was fixed at 10Hz and the stress ratio was set constant at R=0.1. The specimens were conducted at room temperature, 760 °C ,850 °C ,respectively. The stress intensity factor, K is calculated according to the formula from the E647 standard , see equation (2), where $\alpha = a/W$, a is crack length, W and B is 40 and 10mm for this study respectively. ΔP means the external loading range. When the crack length reached 25mm, the test terminated.

$$\Delta K = \frac{\Delta P}{B\sqrt{W}} \frac{(2+\alpha)}{(1-\alpha)^{3/2}} (0.886 + 4.64\alpha - 13.32\alpha^2 + 14.72\alpha^3 - 5.6\alpha^4) \tag{2}$$

Table. 3. Test conditions for specimens

Test Specimens	Temperature °C	Maximum Loading kN	Loading Ratio	Frequency	Ending cycles
L1	RT	8.6	0.1	10Hz	163017 cycles
T1	RT	8.6			341389 cycles
L4	850	8.6			53517 cycles
L5	850	8.6			Fail, 618600 cycles, No Propagation
L6	850	9.4			Fail, 20503 cycles, No Propagation
L9	760	9.4			32919 cycles
T3	760	9.4			31460 cycles
T8	850	10.0			19433 cycles

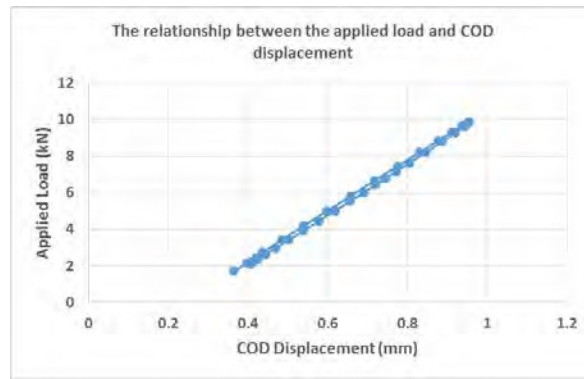


Fig. 3. The relationship between the applied load and COD displacement



Fig. 4. The setup of the elevated temperature

3 Result and discussion

3.1 The fatigue crack growth rates

The overall test results are plotted in the Paris regime, shown in **Fig. 5**. The influence of temperature is obvious, especially for the difference between elevated temperature and room temperature. Meanwhile, the fatigue crack growth (FCG) rate curves were also correlated according to the Paris Law, the result are shown in **Table. 4**. The correlation coefficients have an average of 0.97, which means the curve fits the Paris Law well.

$$\frac{da}{dN} = C(\Delta K)^m \quad (3)$$

Table. 4 Material constant and correlation coefficient for various temperature and orientation

Temperature	Orientation	C	m	R
Room temperature	L	1.63×10^{-11}	4.74	0.99
	T	5.65×10^{-11}	4.34	0.99
760°C	L	3.86×10^{-10}	4.09	0.97
	T	2.17×10^{-8}	2.90	0.97
850°C	L	3.35×10^{-11}	5.05	0.98
	T	3.79×10^{-9}	3.57	0.99

The change of coefficient C and m with the temperature is shown in **Fig. 6**. Both orientation exhibits the same trend in coefficient C and m respectively, but the trends between two coefficients are converse. Coefficient C for orientation T first increased with the growth of temperature. After peaking at the 760°C, it dropped. Whereas, coefficient m for orientation T first decreased and then reached its bottom at 760°C before increased at 850°C. In addition, the coefficient C for orientation T is always higher than that of L, while the coefficient m for orientation T is much lower than L. It seems to be that the coefficient m and C are independent of the temperature for both directions.

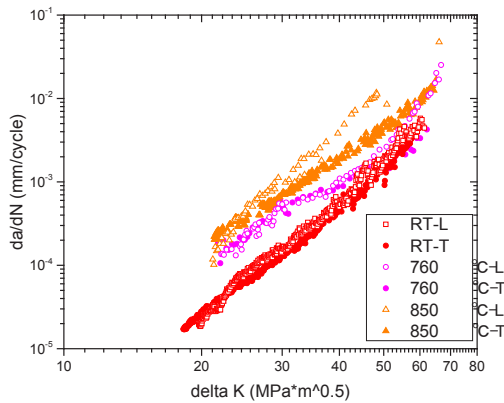


Fig. 5. The da/dN - ΔK curve of six specimens

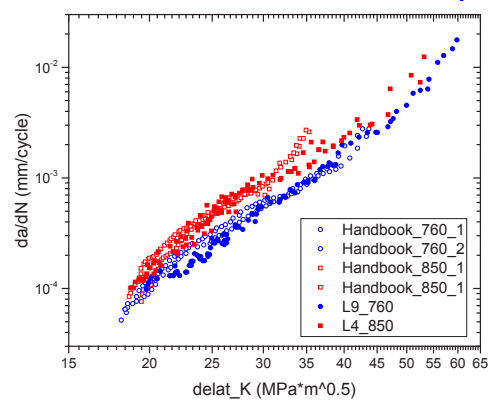


Fig. 7. The comparison between the curve from test and handbook

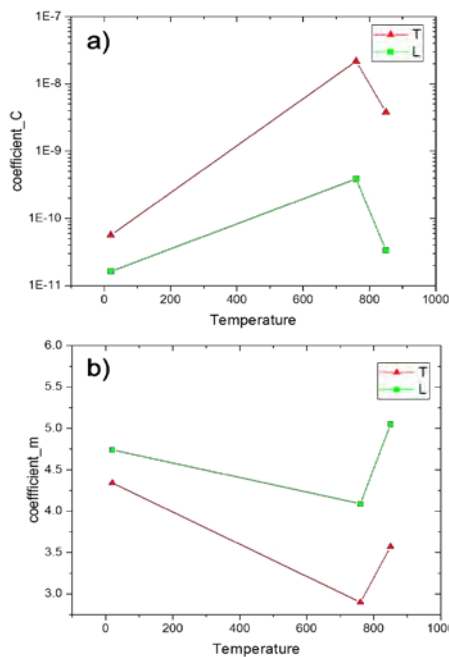


Fig. 6. The relationship between temperature and coefficients, a) C, b) m

Fig. 7 shows the comparison between parts of the test results and handbook data^[11]. The hollow points represent the data collected from the handbook. The test points are almost consistent with the presented data in the medium and high ΔK area, which also means that the result obtained by compliance method is also confident.

3.2 Influence of orientation on FCG rates

Fig. 8 shows the crack growth behavior for T & L orientation at three different temperatures. At the room temperature, the specimen of L exhibited higher FCG rate than that of T through all stages of ΔK , and more specifically the difference seems to be 3-5-times at the medium ΔK level. When it comes to the elevated temperature, there is no such significant difference at lower and medium ΔK level between the L and T orientation. However, for 760°C, in higher ΔK level, the FCG rates between orientation L and T separate obviously. The FCG rate of L is much higher than that of T at the same stress intensity factor, which is not observed in other temperature. The orientation seems to less influence the FCG rates with the increase of temperature. For 850°C, the gap between red curve and blue curve in higher ΔK level is reduced compared with 760°C. In general, the FCG rates of L orientation is higher than T at the three test temperature. However the difference becomes slighter with the increase of temperature, except the obvious difference in higher ΔK level at 760°C. In other words, the influence of orientation of FCG rates is limited at elevated temperature. This is also consistent with other studies: Shi^[12] studied the directionally solidification nickel based superalloys PW1484 at high temperature and pointed that the effect of orientation on the crack propagation is very small. Yoon^[13] also founded that for the GTD-111 the orientation dependence was marginal at the temperature of 649, 761 or 871°C. Although Yoon did not point out the orientation influence at room temperature, an obvious difference can be found in the corresponding graphs.

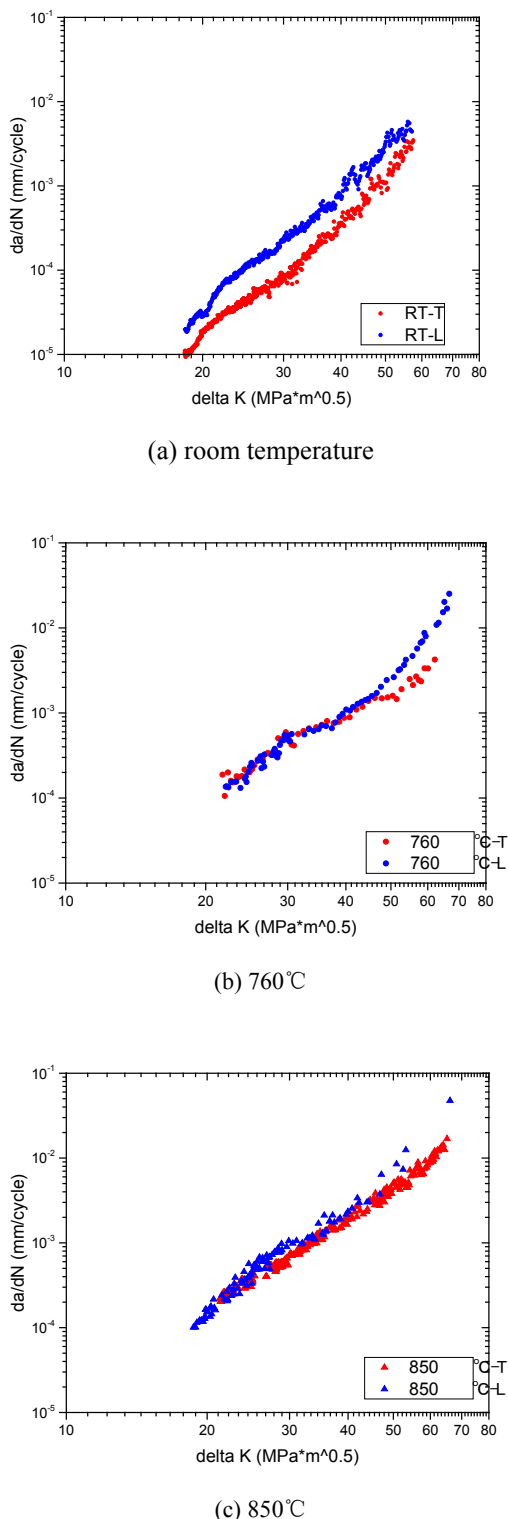


Fig. 8. Influence of orientation on FCG

3.3 Influence of temperature on FCG rates

Fig. 9 shows the FCG rates of cracks for orientation L. The temperature dependence is strong at low and medium ΔK level. The elevated temperature seems to accelerate the FCG rates 10 times larger than that at room temperature. However, in the higher stress intensity factor, the FCG rate at the room temperature

even slightly exceeds that at 760 °C. For high temperature, 90 °C's increase can also exhibit obvious difference. As shown in Fig. 9, the curve for 850 °C is always above the curve of 760 °C and room temperature. Even in the higher stress intensity level, there is no trend of FCG rates reduction.

For the orientation T, similar temperature independence can be found. This also indicates the weak orientation dependence. The FCG rates of 850 °C is still the highest than any other temperature through all the ΔK level. Meanwhile, at higher ΔK level, the FCG rates of room temperature 'caught up' that of 760 °C.

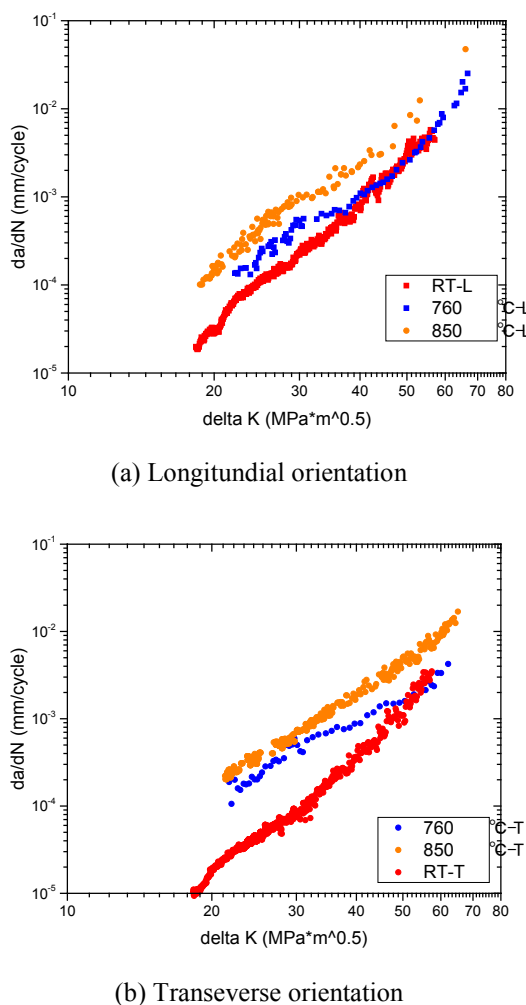


Fig. 9. Influence of temperature on FCG

In conclusion, the increase of temperature can exert strong influence on FCG rates, which speeds up the crack propagation. However, even the room temperature can still have higher FCG rate than 760 °C in higher ΔK level. Generally speaking, high temperature is likely to activate the dislocation motion. And it is also postulated that higher temperature will cause more oxidation, which degraded the material resistance and thus increasing the FCG rates. The reason for the 'collapse' for 760 °C in higher stress level is likely to be the crack closure effect induced by the oxidation. However, it seems to be paradox for the trend observed at 850 °C. Perhaps the

reason for accelerating the FCG rates is determined by other factors. For 760°C, the crack closure plays a more leading role and thus decreasing the FCG rates in higher stress intensity factor level. While for 850°C, the crack closure effect seems to be weak compared with others, thus the curve of lower temperature fails to exceed 850 °C in higher ΔK level.

In the test process, high temperature is also likely to influence the fatigue crack growth threshold. As is shown in **Table. 3** two tests of specimens L5 and L6 could last 20503 and 617600 cycles without any signal of propagation. However, under the same test condition, specimens L4 only took 53517 cycles to the length of 25mm which was set as the terminal condition. For L5 and L6 specimens, we also examined the CT specimens under optical microscope and no sign of propagation can be found. Therefore, we inferred that the threshold is might larger than that of room temperature. The maximum load for L6 was 0.8kN larger than that of L4, L5 and other specimens conducted at room temperature before. In the subsequent tests, the temperature was adjusted to 760°C with maximum 9.4kN. For tests of L9 and T3, approximately 35000 cycles were consumed before reaching the terminal condition and no ‘not propagation’ phenomenon were observed with higher maximum loading. It is hypothesized that the crack closure induced by oxidation is more serve than that at room temperature, and thus increase the threshold level. Telesman^[14] reported that the fatigue crack growth threshold for a PM nickel based superalloy was influence by temperature and frequency. The increase of temperature will lead to the increase of threshold value. Bouvard^[15] and K.S Chan^[16] also mentioned that the thickening of oxide layer on the crack lips tends to increase the opening threshold. However, at present we still lack some evidence to confirm that the oxidation in the main cause for this. In addition, it is also hard to explain the test for L4 whose maximum force was 8.6kN. Further efforts should be made to investigate by studying the fractography under SEM.

4 FCG mode

All the test specimens were separated into two parts shown in **Fig. 10**. For specimens at room temperature, all the crack paths were perpendicular to the loading direction, which satisfies the type I crack growth. However, at the elevated temperature, deflections can be observed in all directions at different high temperature. For L specimen under 760 °C, the crack path grew upward with a certain angle, while the counterpart of T exhibited a ‘strange’ and downward path. At 850°C, L and T specimens travelled in a similar downward path. From the result, it seems that both orientation and temperature could change the fatigue crack growth path. The crack path belongs to the type I-II combined mode. Therefore, the fatigue crack growth path can also to some extent reflect the influence of temperature. The reason for this deflection is likely to be that thermal activated some mechanism and leads to the crack did not travel perpendicularly to the loading direction. And it is

also likely to be caused by the barrier of grain in the crack advancing. In other words, the effect of column grain boundary in the FCG process in unneglectable at elevated temperature. More detailed study should be conducted to confirm it.

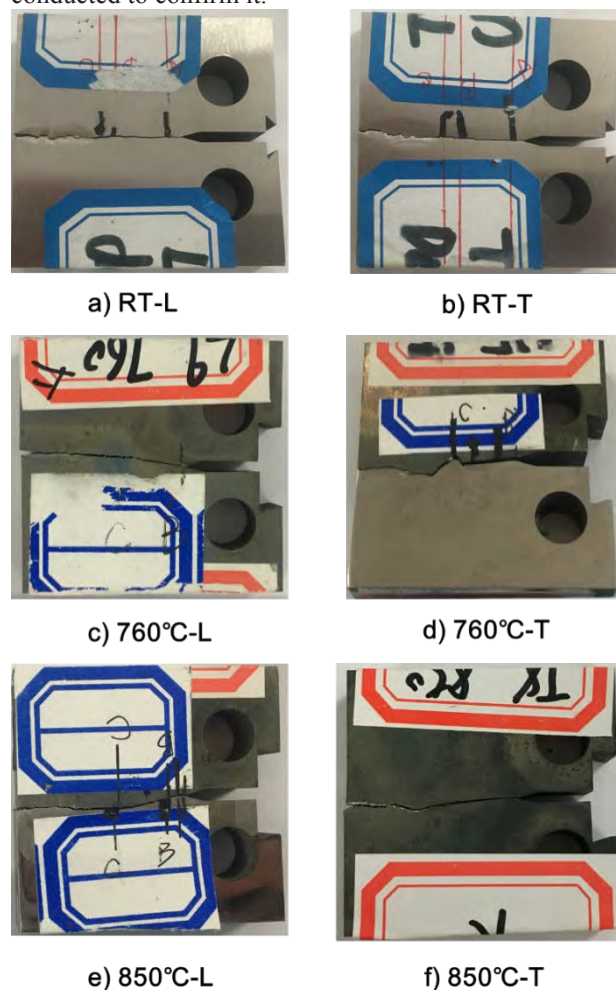


Fig. 10. The FCG path of CT

5 Conclusion

The influence of temperature and orientation on the fatigue crack growth behavior of directionally solidification superalloys named DZ125 have been investigated in this study. Six CT specimens fall into two orientation (longitudinal and transverse) or three temperature (room temperature, 760°C, 850°C). Relevant conclusions are given below:

- 1) The orientation influence seems to be most evident at room temperature, and the temperature effect becomes less significant in low and medium ΔK level with the increase in temperature. For room temperature, 760°C and 850°C, orientation L exhibits slightly higher FCG rates than that of T.
- 2) The increase of temperature accelerated the FCG rates and the difference between the room temperature and elevated temperature is almost an order of magnitude. However, at higher ΔK level, the curve of room temperature could exceed that of 760 °C for both orientations, which is mainly contributed

by the crack closure effect.

- 3) The fatigue crack growth threshold is also likely to be influenced by the increasing temperature, and it is also hypothesized that oxidation is responsible for this.
- 4) The fatigue crack growth path is different from room temperature and elevated temperature. Both L and T orientation travelled perpendicularly to the loading direction which belongs to the type I crack at room temperature while they both exhibited the combined type I-II crack growth mode at elevated temperature.

References

1. M.Qiao,C.Zhou, Corros. Sci.,**63(10)**, 239-245 (2012)
2. D.Shi,J.Liu,X.Yang,H.Qi,J.Wang, Mater. Sci. Eng. A, **528(1)**,233-238 (2010)
3. J.Liang,A.Xing,Z.Wen,Z.Yue, Eng. Failure Anal., **59**,326-333 (2015)
4. X.Hu,D.Shi,X.Yang, Mater. Sci. Eng. A, **674**,451-458 (2016)
5. S.Li,X.Yang,G.Xu,H.Qi,D.Shi, Int. J. Fatigue., **84**,91-96 (2016)
6. T.Liang,H.Guo,H.Peng,S.Gong,Chin.J.Aeronaut., **25(5)**,796-803 (2012)
7. ASTM International. *Standard test method for measurement of fatigue crack growth rates E647-15* (2015)
8. J.Renart,J.Vicens,S.Budhe,A.Rodriguez-Bellido,J.comas, Int. J. Fatigue., **82**, 634-642 (2016)
9. D.Ewest,P.Almroth,B.Sjodin,K.Simonsson,D.Leidermark, Int. J. Fatigue., **92**, 61-70 (2016)
10. B.Pan, Acta Opt. Sin., **31(2)**, (2011)
11. China aviation material manual editorial board , *China aeronautical material manual second volume superalloy casting high temperature alloy* (2002)
12. X.He,Y.Zhang,H.Shi,J.Gu,C.Li, Mater. Sci. Eng. A, **618**,153-160 (2014)
13. K.Yoon,T.Park,A.Saxena, Stren. Fract. & Complex., **4(1)** (2005)
14. J.Telesman,T.Smith,T.Gabb,A.Ring, Mater. Sci. Eng. A,**708** (2017)
15. J.Bouvard,F.Gallerneau,P.Paulmier,J.Chaboche, Int. J. Fatigue., **38(5)**,130-143 (2012)
16. K.Chan,High.Temp.Technol.,**33(4-5)**,425-438 (2016)